BDNF-regulation of *in vivo* axonal transport is selectively impaired in fast motor neurons in SOD1^{G93A} mice.

Andrew P. Tosolini [1, 2], James N. Sleigh[1, 2, 3], Sunaina Surana[1, 2, 3], Elena R. Rhymes [1, 2], Stephen D. Cahalan [4], and Giampietro Schiavo[1, 2, 3]

@AndrewTosolini @J_N_Slayer @sunaina_surana @ellierhymes @Stephen_Cahalan @SchiavoMNPlab

[1] Department of Neuromuscular Diseases, Queen Square Institute of Neurology, University College London, UK. [2] UCL Queen Square Motor Neuron Disease Centre, University College London, UK. [3] UK Dementia Research Institute, University College London, UK. [4] Comparative Neuromuscular Disease Laboratory, Department of Clinical Sciences and Services, Royal Veterinary College, University of London, UK.

Background

Axonal transport ensures long-range, bidirectional delivery of essential cargoes, such as mitochondria, autophagosomes and signalling endosomes, between proximal and distal compartments of neurons for neuronal homeostasis, function and survival (Sleigh et al., 2019; PMID: 31558780). SOD1^{G93A} mice show *in vivo* deficits in axonal transport pre-symptomatically suggesting that axonal transport impairment contributes to disease (Bilsland et al., 2010; PMID: 21059924). Brain-derived neurotrophic factor (BDNF) is critical for neuronal development and synaptogenesis; however, in adulthood its expression is reduced, and BDNF functions to mediate neuronal survival in a variety of neurons, and synapse maintenance, including at the neuromuscular junction (NMJ). α-motor neurons (MNs) are defined by the type of muscle fibre they innervate; α-MNs innervating tibialis anterior (TA) are comprised of fast-fatiguable (FF) and fast-fatigue resistant (FFR) subtypes, and α-MNs innervating soleus are comprised of slow-fatigue resistant (SFR) (Stifani, 2014; PMID: 25346659). In SOD1^{G93A} mice, fast-fatiguable motor neurons (e.g., innervating TA) are more vulnerable than slow-fatigue resistant motor neurons (e.g., innervating soleus) (Pun et al., 2006; PMID: 16474388). As the influence of both α-motor neuron subtype and BDNF regulation on axonal transport are currently unknown, determining the mechanisms that regulate BDNF-signalling in motor neuron subsets, as well as in disease, will reveal novel clues about pathomechanisms influencing selective motor neuron vulnerability in ALS.

Objectives

1) Evaluate basal axonal transport dynamics in different muscle subtypes; and whether transport is influenced by BDNF stimulation.
2) Characterise BDNF levels in skeletal muscles and at the NMJ.
3) Assess alterations in SOD1^{G93A} pathology.

Methods

Axonal transport was visualised *in vivo* with intramuscular injections of fluorescently-labelled atoxic fragment of tetanus neurotoxin (H_CT). H_CT was delivered into TA or soleus muscles of wild-type (WT) and SOD1^{G93A} mice (at time points that correspond with ~20% (P73) and ~40% (P94) loss of MNs), +/- 25 ng of recombinant BDNF (Sleigh et al., 2020; PMID: 32524487). 4+ hours later, sciatic nerves were exposed in live, anaesthetised animals, and imaged using time-lapse confocal-microscopy at 37°C. Retrogradely transported, H_CT-labelled signalling endosomes within single axons were tracked using TrackMate (Tinevez et al., 2006; PMID: 27713081). Muscle and sciatic nerve BDNF, receptors, and signalling pathways expression were assessed in SOD1^{G93A} mice and age-matched, WT littermates by immunoblotting. TrkB and p75^{NTR} levels were assessed via immunohistochemistry on NMJs from teased muscle fibres or sciatic nerve cryosections.

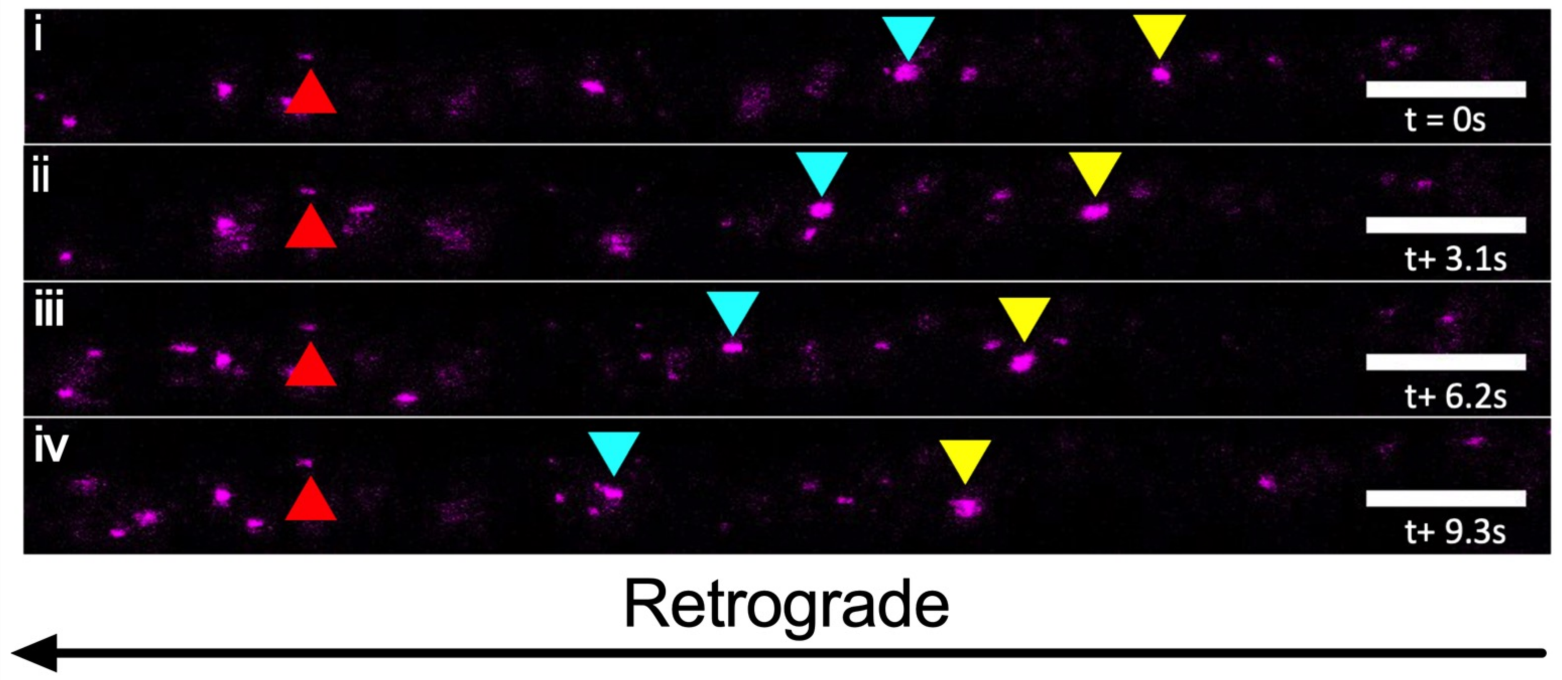

Figure 1. Representative image series acquired by intravital time-lapse confocal microscopy of retrogradely transported (i.e., right-to-left) HcT-555+ signalling endosomes (purple) from a single sciatic nerve axon in a live, anaesthetised mouse. *i-iv)* Four consecutive frames (frame rate=3.1 s) highlighting the axonal transport dynamics of three representative HcT-555+ signalling endosomes. Yellow and cyan arrows are examples of retrograde moving signalling endosomes, whereas red arrows signify a paused signalling endosome. Scale bar = 10µm. The output of this analysis provides information on individual cargo including frame-to-frame and overall track velocities and displacement. ≥1000 endosome steps from a total of 15-30 endosomes across ≥3 axon bundles were analysed/animal.

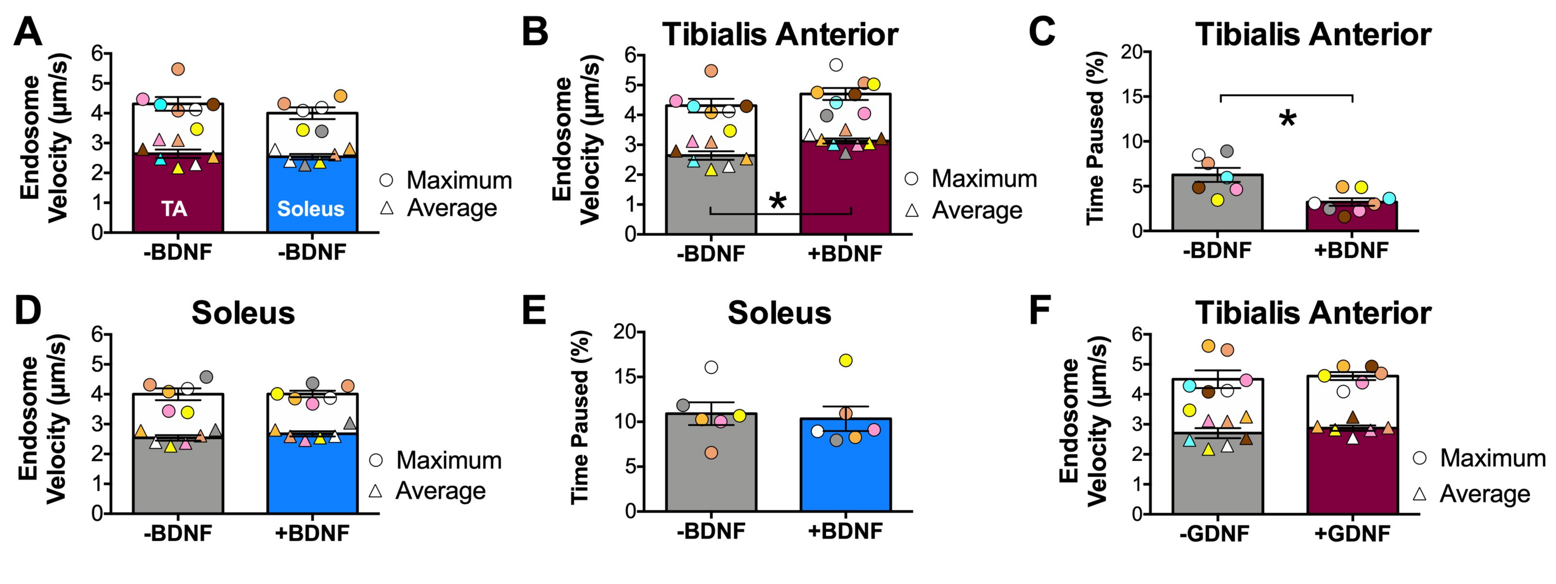

Figure 2. BDNF selectively enhances *in vivo* axonal transport dynamics in wild-type fast, but not slow motor neurons. A) Basally, fast motor neurons (maroon) innervating tibialis anterior (TA) and slow motor neurons innervating soleus (blue) muscles display similar mean and maximum average axonal transport velocities of signalling endosomes. **B)** BDNF stimulation in fast motor neurons innervating TA enhance mean signalling endosome velocities, with a concurrent **C)** reduction in time that signalling endosomes pause. **D)** However, BDNF stimulation in slow motor neurons innervating soleus does not not enhance mean velocities of signalling endosomes, **E)** nor does it influence pausing dynamics. **F)** GDNF stimulation in wild-type fast motor neurons does not enhance axonal transport dynamics demonstrating phenotypical specificity for BDNF in fast motor neurons. Means ± standard error of the mean (S.E.M.) are plotted for all graphs. Average (Δ) and maximum (O). * p < 0.05, assessed by a two-tailed unpaired t-test/Mann-Whitney U test. n=6-8.

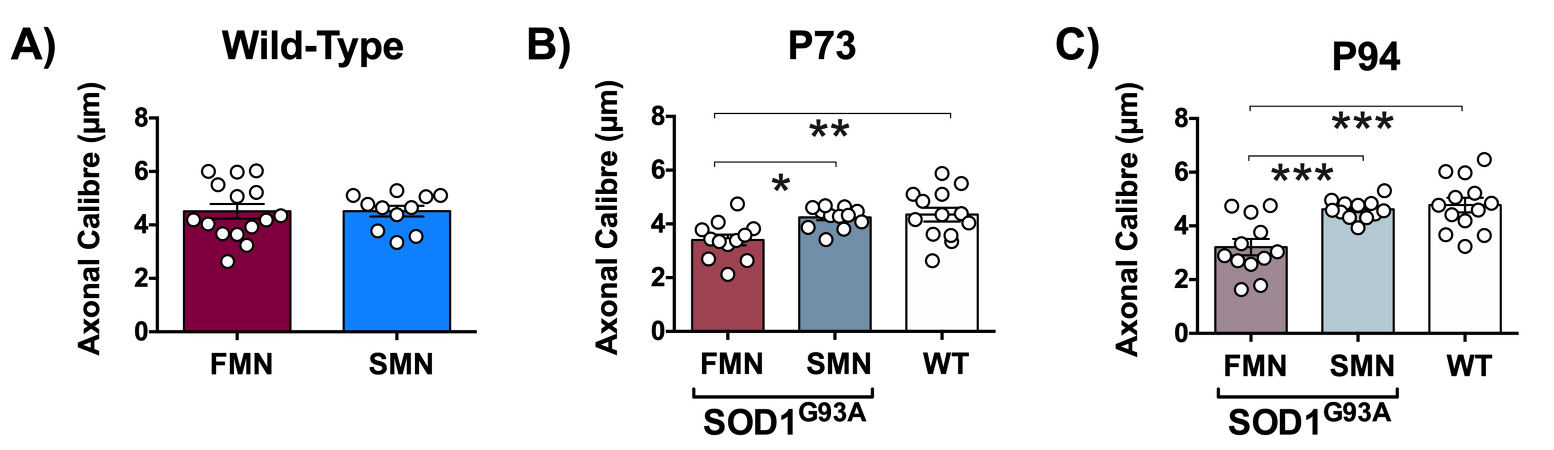

Figure 3. Motor axon calibre is selectively reduced in FMN axons in SOD1^{G93A} mice.
A) There are no differences between FMN and SMN axons in the wild-type (WT). However, there is preferential and progressive reduction in axonal calibre of FMNs in **B)** SOD1^{G93A} mice at P73 and **C)** P94 compared to both SOD1^{G93A} SMNs and age-matched WTs. Means ± standard error of the mean (S.E.M.) are plotted for all graphs. * p <0.05, ** p <0.01, *** p <0.001 assessed by a one-way ANOVA followed by *post-hoc* Tukeys test for multiple comparisons. n=11-15

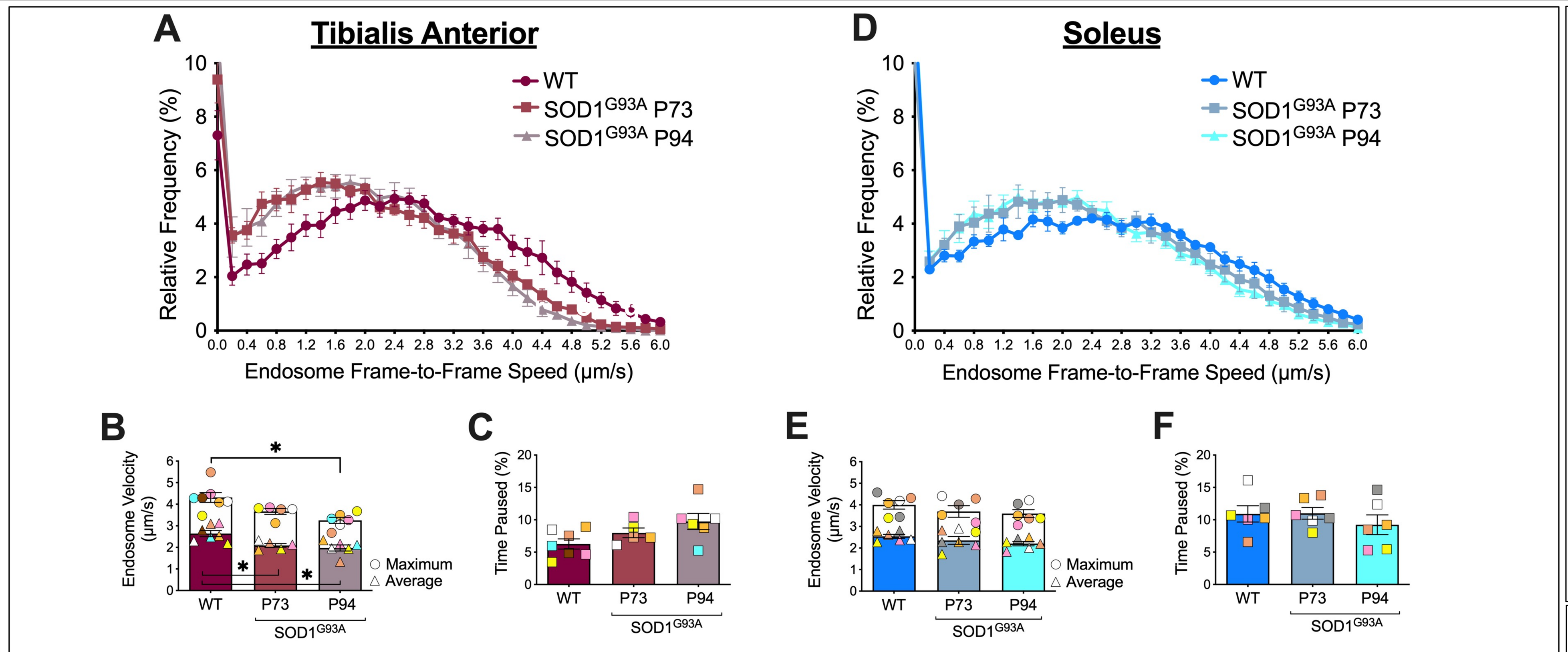

Figure 4. Axonal transport of signalling endosomes in fast motor neurons (FMNs) are selectively impaired in SOD1^{G93A} mice.
A) Speed distribution curves indicating that FMNs innervating Tibialis Anterior display axonal transport dynamics in two stages of SOD1^{G93A} disease compared to wild-type, with **B)** mean and maximum velocities significantly reduced compared to wild-type, and **D)** without any significant alterations in pausing dynamics. **D)** On the other hand, slow motor neurons (SMNs) innervating soleus display no impairments at the same stage of disease, with unperturbed **E)** mean and maximum velocities and **F)** pausing dynamics in SMNs innervating soleus. * p <0.05, assessed by a one-way ANOVA followed by *post-hoc* Tukeys test for multiple comparisons. n=6-8

Tibialis Anterior +BDNF

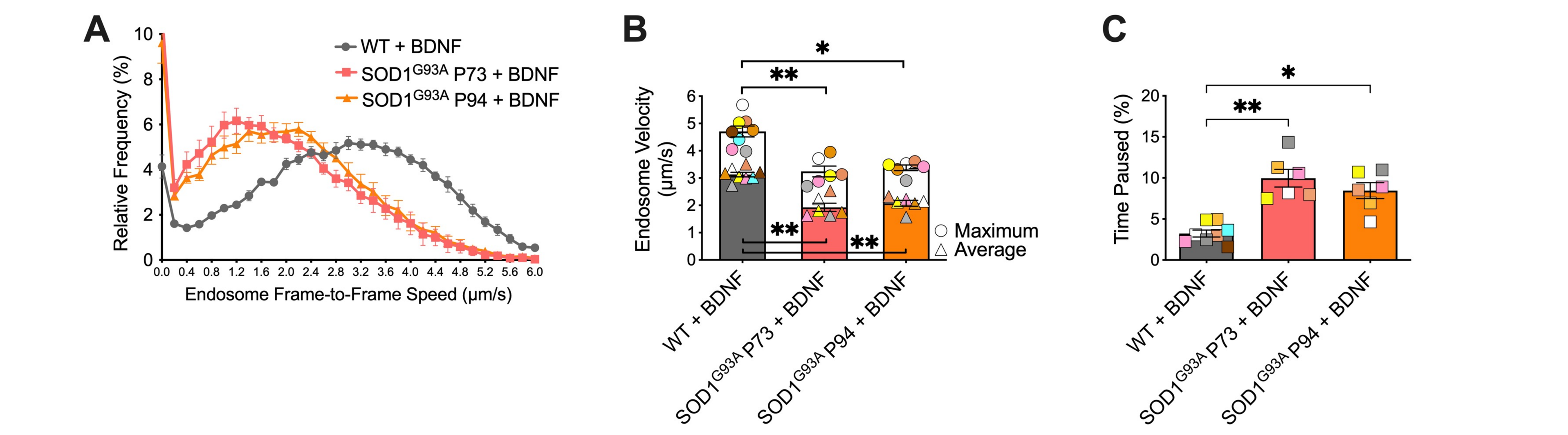

Figure 5. Axons innervating TA become insensitive to BDNF stimulation in SOD1^{G93A} mice.
A) Speed distribution curves of TA axons stimulated with BDNF display striking impairments in transport dynamics in pathological SOD1^{G93A} mice. **B)** When stimulated with BDNF, the mean and maximum velocities are significantly reduced compared to wild-type with **C)** significant increases in pausing dynamics. * p <0.05, ** p <0.01, assessed by one-way ANOVA followed by a Kruskal-Wallis multiple comparisons test. n=6-8.

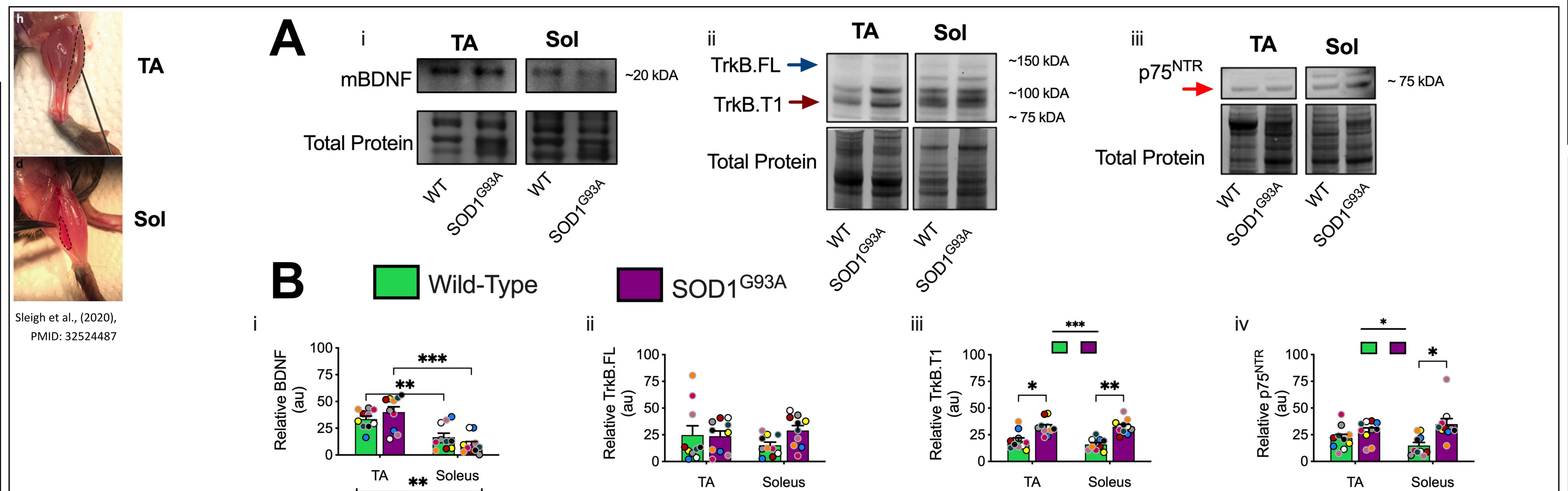

Figure 6. TA has more BDNF irrespective of pathology, but disease increases TrkB.T1 and p75^{NTR} expression in muscles. A) Representative immunoblots of i) mature BDNF (mBDNF), ii) TrkB.FL, TrkB.T1 and iii) p75^{NTR} from WT and SOD1^{G93A} TA and SOL muscles, that are normalised to total protein loading. Lanes 1 & 3: WT; Lanes 2 & 4: SOD1^{G93A}. **B)** Quantifications of i) mBDNF, ii) TrkB.FL, iii) TrkB.T1 and iv) p75^{NTR}. Means ± standard error of the mean (S.E.M.) are plotted for all graphs. * p < 0.05, ** p < 0.01, *** p < 0.001 assessed by two-way ANOVA followed by Holm-Sidak's multiple comparison test. n=10.

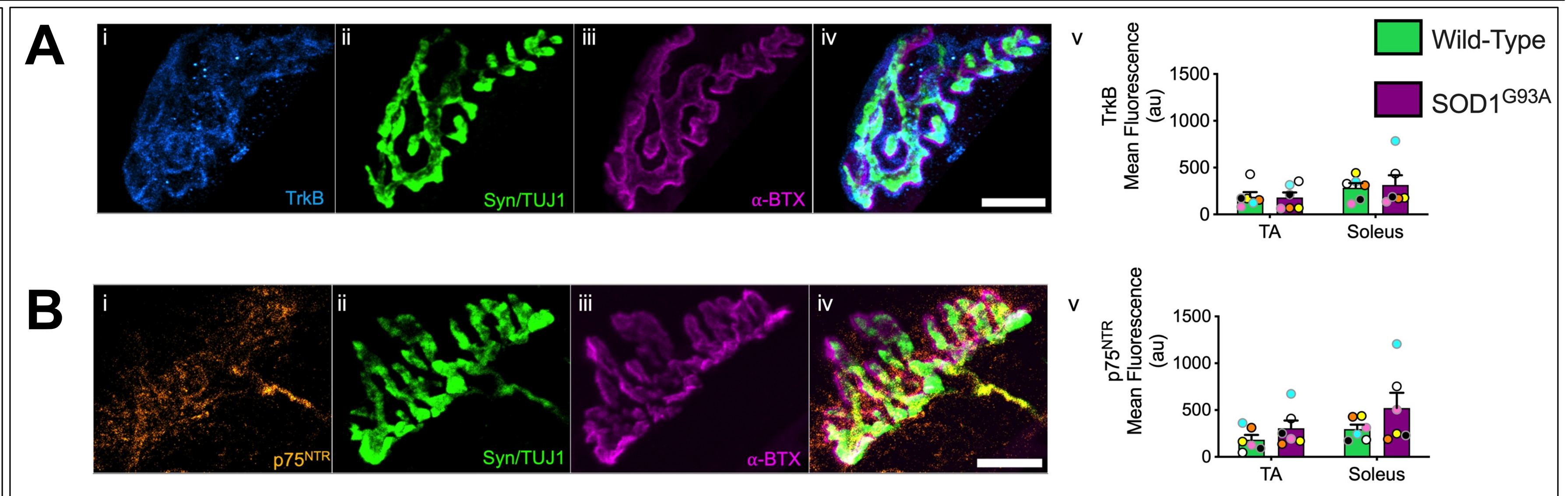

Figure 7. Basal or pathological TrkB or p75^{NTR} receptor expression does not differ in tibialis anterior (TA) or soleus neuromuscular junctions (NMJs). Representative immunohistochemistry of i) **A)** TrkB (blue) or **B)** p75^{NTR} (yellow), ii) Pre-synaptic terminals (Synaptophysin/βIII-Tubulin; green), iii) post-synaptic regions (α-bungarotoxin; magenta), and iv) overlay. Quantifications of mean fluorescence of *v)* **A)** TrkB-positive or **B)** p75^{NTR}-positive NMJs from TA or Soleus indicate no significant differences between in either muscle, basally or in pathology, as assessed by a two-way ANOVA followed by Holm-Sidak's multiple comparison test. n=6

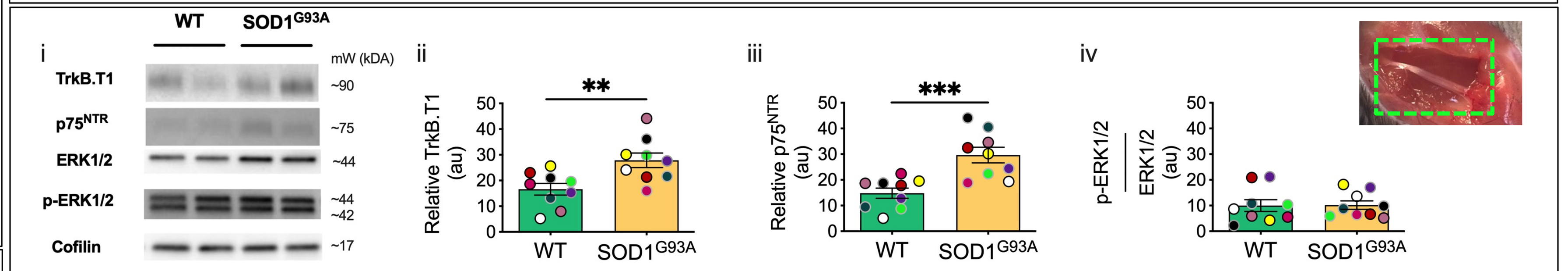

Figure 8. TrkB.T1 and p75^{NTR} expression is increased in sciatic nerves in disease. **A)** Representative immunoblots of TrkB.T1, p75^{NTR}, ERK1/2, and p-ERK1/2 that were normalised to the Cofilin housekeeping gene in sciatic nerves of wild-type and SOD1^{G93A} mice. Quantifications indicating that expression of ii) TrkB and iii) p75^{NTR} but not iv) p-ERK1/2 ratios are increased in SOD1^{G93A} mice. Means ± standard error of the mean (S.E.M.) are plotted. ** p <0.01, *** p <0.001 assessed by an unpaired t-test. n=10

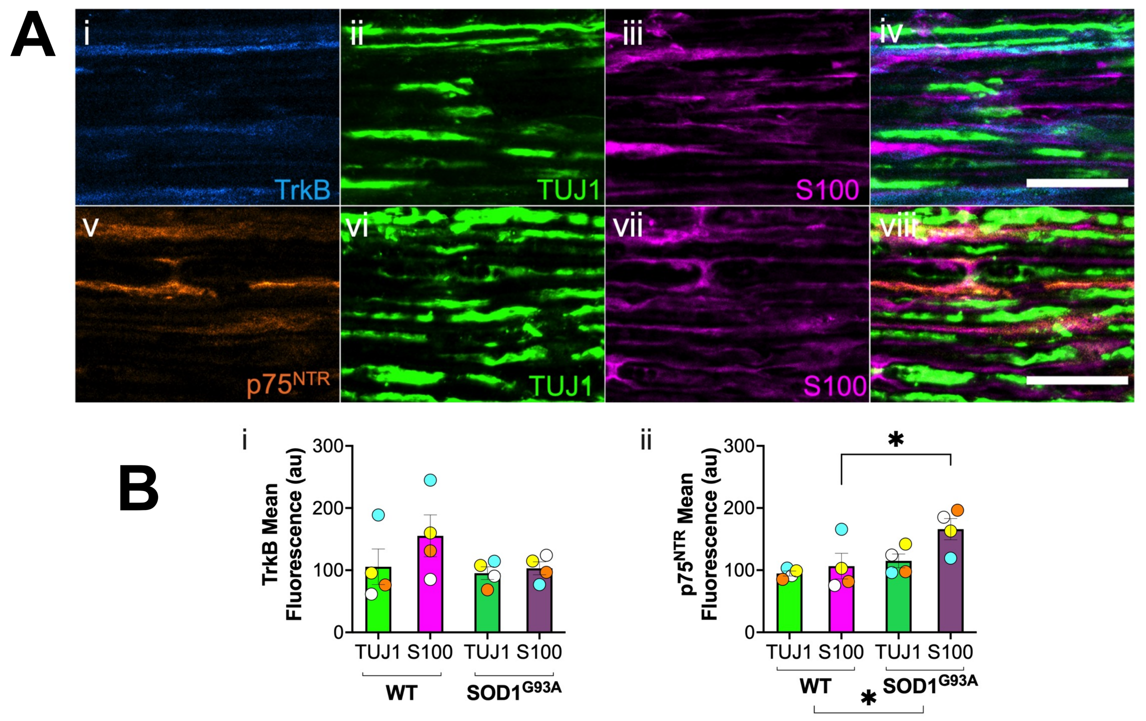

Figure 9. p75^{NTR} expression is increased specifically in Schwann cells in SOD1^{G93A} sciatic nerves.
A) Representative immunostaining of *i)* TrkB (blue) or *v)* p75^{NTR} (orange) receptors; *ii, vi)* axons (TUJ1); green), *iii, vii)* Schwann cells (S100; magenta), *iv, viii)* overlay. Scale bar = 25µm. **B)** Quantifications reveal *i)* similar TrkB receptor expression in axons and Schwann cells, with no pathological alterations in SOD1^{G93A} sciatic nerves. *ii)* On the other hand p75^{NTR} receptor expression is increased in SOD1^{G93A} sciatic nerves, specifically in Schwann cells. * p <0.05, assessed by a two-way ANOVA followed by a Holm-Šídák's multiple comparisons test. n=4.

Discussion

- Basally, FMN and SMN axons have similar axonal transport dynamics of signalling endosomes.
- BDNF enhances axonal transport specifically in fast motor neurons in wild-type mice.
- FMN axons display reduced axon calibre in pathology whereas SMN axons remain unperturbed.
- Axonal transport is selectively impaired in FMNs in SOD1^{G93A} pathology.
- FMN axons become insensitive to BDNF stimulation in pathology.
- BDNF is expressed more in TA basally, and pathology induces increases in TrkB.T1 and p75^{NTR}.
- Pathology does not alter TrkB or p75^{NTR} levels at the NMJ levels of BDNF.
- TrkB.T1 and p75^{NTR} receptor levels increase in SOD1^{G93A} sciatic nerves, specifically in Schwann cells.

Conclusions

These data indicate that different MN/muscle subgroups have distinct axonal transport features, including sensitivity to BDNF stimulation, and that cell and non-cell autonomous BDNF signalling is impaired in SOD1^{G93A} pathology.